contribution. Freeman and Watson[42] have calculated $A^c = -27.5$, $A^L = 56.5$, and $A^d = 4.0$ T for the free ferrous ion. These values may be reduced by covalency effects but will suffice for our purposes. The orbital term arises from electron currents unquenched by spin–orbit coupling and, within our rough model

$$g_x = g_z - (2/\lambda)(D - E) \qquad g_y = g_z - (2/\lambda)(D + E) \quad (6)$$

where λ is the spin–orbit coupling constant and equals -103 cm^{-1} for the free ion.[41] The sign of the spin–orbit interaction is such that $g_p \geq 2$ and the orbital contribution to **A** opposes the contact contribution in all directions. The value and uncertainty of the observed μ_{eff} coupled with the large magnitude of A^L render calculations of the average orbital moment meaningless. Therefore, we simply choose the smallest g_p to equal 2 and proceed to the dipole term. The tensor d_{pq} is proportional to the valence efg, V_{pq}^{val}, with sign (d_{pq}) = sign (V_{pq}^{val}). The quantity $d = d_{zz}(1 + \eta_{val}^2/3)^{1/2}$ will equal ± 2 if the orbital moment is totally quenched. Assuming that the observed efg is proportional to the valence efg and that $d = 2$, we use the D, E/D, and efg of Table VII and calculate from eq 5 $A_x = -20$, $A_y = -11$, and $A_z = -35$ T for reduced Cp Rd and $A_x = -31$, $A_y = -30$, and $A_z = -15$ T for Ia. Comparison with the observed values shows that our crude high-spin ferrous model accounts for the anisotropy of **A** for both Cp Rd and Ia. In contrast, the **A** of high-spin ferric ions are dominated by the contact term with all the A_i typically being within 15% of their average. Hence, the Mössbauer data suggest that the $[S_2MoS_2Fe(SPh)_2]^{2-}$ cluster is more accurately described as $Fe^{2+}Mo^{6+}$ rather than $Fe^{3+}Mo^{5+}$. The small quadrupole splitting and isomer shift of Ia do raise questions concerning the extent of the delocalization of some or all of the iron 3d electrons. However, we hesitate to draw any conclusions concerning this point since the present uncertainty in the orbital term prevents any quantitative comparison of the **A** of Ia with those of other complexes.

A simple linear relationship of isomer shift to average oxidation state has been established for iron in tetrahedral sulfur environments.[6b] For Ia we have observed an isomer shift of 0.43 mm/s at 160 K and estimate $\delta = 0.45$ mm/s at 77 K. After subtracting 0.12 mm/s to correct for our 300 K source temperature, we find that Figure 7 of ref 6b predicts an effective oxidation state of +2.6. However, the similarity of the isotropic parts of **A** for Ia and reduced Rd plus the anisotropy discussed above suggest a more ferrous character. We conclude that a definitive assignment of oxidation state to iron in mixed iron–molybdenum complexes such as Ia is difficult at best and that a simple relationship of isomer shift to such an assignment may not exist.

(42) A. J. Freeman and R. E. Watson, *Phys. Rev.*, **131**, 2566 (1963).

Conclusions

The heterobimetallic species $[S_2MoS_2FeX_2]^{2-}$ (X = Cl, aryl thiolate) are readily prepared and interconverted. Analysis of magnetic susceptibility and Mössbauer data suggests a high-spin Fe(II)–Mo(VI) formulation. The dimensions and chemical reactivity of the MoS_2Fe core are comparable to those found in complexes containing the Fe_2S_2 core. Most importantly, the MoS_2Fe unit exhibits a stability comparable to that of the $MoFe_3S_4$ substituted cubane, and thus must also be considered as a potential structural fragment in the FeMo cofactor of nitrogenase.

Acknowledgments. This research was supported by grants to B.A.A. from the National Science Foundation (CHE-7715990) and the USDA/SEA Competitive Research Grants Office (5901-0410-8-0175-0) and by grants to E. Münck from the National Science Foundation (PCM77-08522) (T.A.K.) and the National Institutes of Health (GM22701) (B.H.H.). H.C.S. was supported by a General Electric Co. Summer Fellowship (1979). We thank E. Bouhoutsos-Brown for assistance with the NMR spectra and E. Münck for helpful discussions. We are grateful to Dr. F. J. DiSalvo at Bell Laboratories for assistance with and discussions on the temperature-dependent susceptibility data.

Supplementary Material Available: Positional and thermal parameters (Table VIII), interatomic distances (Table IX), and bond angles (Table X) for the cations (3 pages). Ordering information is given on any current masthead page.

Phosphorus-31 Spin–Lattice Relaxation in Aqueous Orthophosphate Solutions[1]

Douglas C. McCain*[2] and John L. Markley

Contribution from the Department of Chemistry, Purdue University, West Lafayette, Indiana 47907. *Received February 14, 1980*

Abstract: Phosphorus-31 spin–lattice relaxation rates and nuclear Overhauser enhancements were measured for sodium orthophosphate in aqueous solution as a function of pH, temperature, concentration, magnetic field strength, and percent deuterium in the solvent. We demonstrate that relaxation easily can be dominated by trace impurities of transition-metal ions. In rigorously purified samples, the longitudinal relaxation rate is nearly independent of pH or concentration. The longitudinal relaxation rate has been resolved into contributions from dipole–dipole, chemical shift anisotropy, and residual components. The results support an ion–solvent interaction model in which the PO_4 group is locked into the local water structure by numerous hydrogen bonds. We propose a hydrogen-bond shift mechanism, termed "quasi-rotation", which accounts for the observed chemical shift anisotropy relaxation rate. Proton tunneling appears to influence chemical shift anisotropy relaxation in H_2O but not in D_2O at low temperatures. We suggest that the residual relaxation component which has a positive activation energy arises from "quasi-spin rotation" resulting from hydrogen-bond shifts.

Introduction

Phosphorus-31 nuclear spin relaxation in aqueous orthophosphate solutions has been the subject of several publications.[3-9] Some of the literature data have been replotted in Figure 1 as ^{31}P spin–lattice relaxation rates, $1/T_1$, vs. pH. There is general

(1) Presented at the Great Lakes Regional Meeting of the American Chemical Society, Rockford, Ill., June 1979.

(2) Department of Chemistry, Southern Station Box 9281, University of Southern Mississippi, Hattiesburg, Miss. 39401.

(3) W. E. Morgan and J. R. Van Wazer, *J. Am. Chem. Soc.*, **97**, 6347 (1975).

0002-7863/80/1502-5559$01.00/0

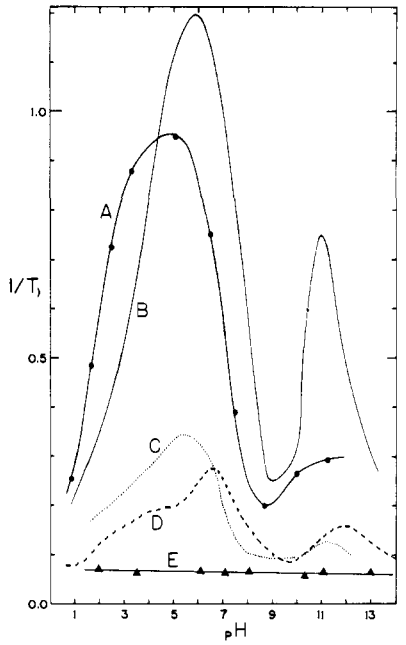

Figure 1. ^{31}P relaxation rate (s^{-1}) vs. pH in orthophosphate solutions at about 30 °C. These curves illustrate the large discrepancies between the present results with highly purified orthophosphate and those published previously. Curve A, 0.3 M in H_2O, Na^+ counterion, passed through Chelex, then 1.0 ppm Fe^{3+} added, 24.3 MHz, 32 °C, this work; B, 1.0 M in H_2O, Na^+ counterion, no purification, 24.29 MHz, 25 °C, redrawn from Figure 1 in ref 5; C, 0.2 M in 20% D_2O, Na^+ counterion, treated with "excess" Chelex, 109.3 MHz, unspecified temperature, redrawn from Figure 1 in ref 6; D, 0.2 M in H_2O, $N(CH_3)_4^+$ counterion, no purification, 40.5 MHz, 31 °C, redrawn from Figure 1 in ref 3; E, 0.1 M in 20% D_2O, Na^+ counterion, passed through Chelex, 60.74 MHz, 30 °C, this work.

agreement among previous authors that $1/T_1$ is a strong function of pH, but it is also clear from Figure 1 that data obtained in different laboratories are not ideally reproducible.

This paper reports new data demonstrating that earlier pH-dependent results were governed by trace concentrations of transition-metal ions. We show that $1/T_1$ is almost independent of pH in rigorously purified samples. We have also resolved the contributions of individual relaxation mechanisms to the overall spin–lattice relaxation rate, allowing us to analyze the solution dynamics of orthophosphate ions and to propose a solvation model that explains our results.

Experimental Section

NMR Spectrometers. Four different FT NMR spectrometers were used for this work. Most of the data were obtained with a Nicolet Technology Corp. NT-150 operating at a ^{31}P frequency of 60.74 MHz. An NT-360 at 145.75 MHz and a modified XL-100 at 40.51 MHz were used to measure relaxation rates as a function of field. A home-built spectrometer[10] at 24.3 MHz was used for some preliminary measurements. The Nicolet instruments have quadrature detection, 32K memory, deuterium internal lock, and computer-controlled variable-temperature air flow. Estimated maximum temperature errors at the sample were ±2 °C. All samples were 12 mm in diameter and >10 cm deep, except those studied at 24.3 MHz, which were held in spherical inserts. A 20-mm probe was used on the NT-150 for best rf field homogeneity; the other spectrometers were fitted with 12-mm probes.

Sample Preparation. For these measurements it is absolutely essential that all paramagnetic impurities be reduced to the lowest possible levels. This was accomplished by passing phosphate solutions through a chelating cation exchange resin. Typically, a glass column (25 × 2.2 cm) was packed with a slurry of Chelex-100 (Bio-Rad Laboratories, Na^+ form at pH 10). To make a typical sample, 10 mL of 0.25 M Na_2HPO_4 (reagent grade) was loaded on the column. Upon elution with distilled, deionized water, a 20-mL fraction containing the phosphate band was collected and mixed with 5 mL of D_2O (Bio-Rad, 99.8% D) to make a solution containing 0.10 M Na_2HPO_4 in 20% D_2O at about pH 10.3. Samples were placed in 12-mm glass NMR tubes which had been washed in HCl, soaked in EDTA solution, and rinsed with Chelex-treated water; they were deoxygenated by bubbling with N_2, although tests without N_2 showed no significant decrease in relaxation times. To make the samples in 100% D_2O, some of the purified fractions were lyophilized and then redissolved in D_2O. In comparing D_2O as purchased from Bio-Rad with D_2O that had been treated with deuterium-exchanged Chelex-100, no difference in relaxation times was found. To investigate ionic strength and concentration effects, samples were prepared at 0.010 or 0.10 M Na_2HPO_4; ultrapure NaCl (Alfa Inorganics) was added to some of the samples to make solutions at 0.10 M Na_2HPO_4 be also 0.30 M in NaCl. Some preliminary work was done with 0.30 M Na_2HPO_4. To lower the pH, samples were titrated with ultrapure HCl (Alfa Inorganics); the pH was measured on a Corning Model 112 pH meter. The sample at pH 13 was prepared by adding sufficient solid NaOH and Na_2S (reagent grade) to a sample of 0.10 M Na_2HPO_4 to make the solution contain 0.10 M Na_3PO_4, 0.10 M NaOH, and 0.001 M Na_2S. Sulfide removes trace metal contaminants in NaOH. The pH of this solution was assigned by calculation, not measurement. One D_2O sample at pH 10.2 was made with an equimolar mixture[11] of $P^{16}O_4^{3-}$ and $P^{18}O_4^{3-}$. Glass electrode pH meter readings in D_2O were not corrected for the deuterium isotope effect.

Out of 16 samples at pH 10, two, for no apparent reason, showed unusually short T_1 values. When a small amount of Na_2EDTA was added (to make ca. 10^{-3} M), the relaxation times increased to about the same value as in the other 14 samples; we may assume that somehow these samples had been contaminated. Tests with EDTA added to the other samples showed no change in T_1. Our confidence in sample purity is based on excellent T_1 reproducibility (except for the two contaminated samples) and the fact that our T_1 values are as long as or longer than any that have been reported previously for orthophosphate solutions (see Figure 1). If contamination were a general problem, we would expect erratic results from all samples and shortened T_1 values, especially near the positions of the peaks in Figure 1.

Tests with trace amounts of added ferric ion (1.0 ppm Fe^{3+}) showed slightly shortened T_1 values over the pH range 8–10 and much shorter T_1 values from pH 3 to 7; the excess relaxation rate due to this amount of ferric ion is ca. 0.05 s^{-1} at pH 5 (see Figure 1). Similar results have been observed[6] with added cupric ion.

Some of the pH 10 samples were kept for long periods of time. After more than 1 month's storage, the T_1 began to drift to shorter values, perhaps because transition-metal ions leach from the glass NMR tubes.

Experimental Procedure. Samples placed in the spectrometer were allowed to reach thermal equilibrium. Approach to equilibrium is easily monitored; at 60.74 MHz the ^{31}P resonance frequency shifts by about 1 Hz/deg, partly owing to a shift in the deuterium lock resonance. The spectrometer carrier frequency was set to within 100 Hz of the ^{31}P resonance, and the 90° pulse width was determined to within ±2°. (On the NT-150 a 90° pulse is 36 ± 4 μs.) For each sample, and at each new temperature, the 90° pulse was redetermined. T_1 measurements used the inversion–recovery pulse sequence $(PD-180°-\tau-90°-FID)_x$, where PD is a pulse delay (PD > $4T_1$), and $x = 1$ (except $x = 4$ for 0.01 M samples), and with 7–32 (usually 14) different τ values. Each free induction decay (FID) was apodized exponentially and Fourier transformed, and the highest points on the resonance curve were fitted to a quadratic function in order to compute a corrected peak height, $S(\tau)$. These data were then fitted to the function[12]

$$S(\tau) = S(\infty)\{1 - (1 + W(1 - e^{-PD/T_1})e^{-\tau/T_1})\} \quad (1)$$

The W term partially corrects for errors in pulse angle and effects of inhomogeneous rf fields. Typical W values were 0.9 on the NT-150 and 0.7 on the other instruments. Inclusion of PD in the function compensates for the ca. 4% errors expected when PD = $4T_1$. Successive T_1 measurements on any sample without changing temperature agreed to within ±3%; simultaneous but independent T_1 measurements on the two resolved peaks in the $P^{16}O_4^{3-}/P^{18}O_4^{3-}$ sample gave identical results within ±1% standard deviation.

(4) T. Glonek and J. R. Van Wazer, *J. Am. Chem. Soc.*, **80**, 639 (1976).
(5) H. S. Kielman and J. C. Leyte, *Ber.*, **79**, 1201 (1975).
(6) J. Granot, G. A. Elgavish, and J. S. Cohen, *J. Magn. Reson.*, **33**, 569 (1979).
(7) G. A. Elgavish and J. Granot, *J. Magn. Reson.*, **36**, 147 (1979).
(8) P. L. Yeagle, W. C. Hutton, and R. B. Martin, *J. Am. Chem. Soc.*, **97**, 7175 (1975).
(9) T. Glonek, *J. Am. Chem. Soc.*, **98**, 7090 (1976).
(10) In the laboratory of Dr. M. P. Klein, University of California, Lawrence Berkeley Laboratory, Berkeley, Calif.
(11) Labeled phosphate donated by Dr. R. L. Van Etten was prepared as described by J. M. Risley and R. L. Van Etten, *J. Labelled Compd. Radiopharm.*, **15**, 533 (1979).
(12) G. C. Levy and I. R. Peat, *J. Magn. Reson.*, **18**, 500 (1975).

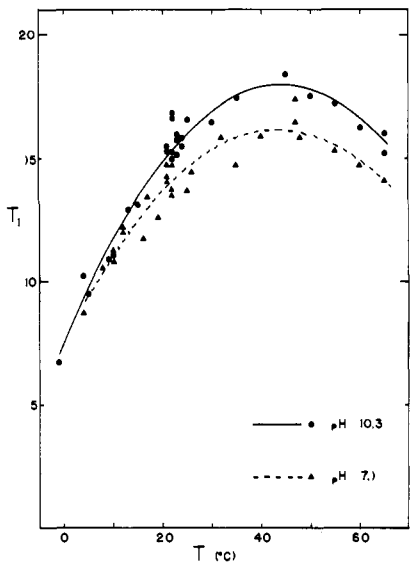

Figure 2. T_1 (s) vs. temperature for sodium orthophosphate solutions in 20% D_2O measured at 60.74 MHz. Data points represent individual measurements; lines are the least-squares quadratic fit.

Nuclear Overhauser effect (NOE) measurements used the gated decoupling technique[13] with pulse delays $>10T_1$. The decoupler was set very near the proton frequency and square wave modulated at 50–100 Hz. Power levels of 1–15 W were tried, but data from the higher power levels have been discarded because of sample heating problems. At 1.5 W (the usual level) a 1–2 °C temperature rise was measured by using the ^{31}P resonance frequency as an internal probe. Data from different power levels indicate that at ca. 1 W the NOE effect is saturated. The NOE enhancement factor, η, is defined as

$$\eta + 1 = S(\text{on})/S(\text{off}) \quad (2)$$

where S(on) and S(off) refer to corrected peak heights with decoupler on and off, respectively. Reported values are the average of five to nine successive determinations.

Data Reduction. From 30 different samples, this study produced hundreds of data points, each point defined by seven variables: T_1, η, pH, temperature, concentration, magnetic field, and % D in the solvent. Data analysis requires a combination of information from each variable. To simplify this task, data points were fitted to appropriate functions, using a least-squares procedure. T_1 was treated as a polynomial function of temperature. Figure 2 shows some typical results. The quadratic function, although arbitrary, gives an excellent fit; functions with higher powers of temperature or other elaborations are not significantly better. NOE data were fitted to a linear function of temperature as shown in Figure 3. Within experimental error, results for both T_1 and NOE are independent of concentration or ionic strength in the ranges studied. Results are also insensitive to pH. For this reason, statistical accuracy in the least-squares fit can be improved by combining data for all concentrations to increase the number of points. Also, some data from different pH values have been combined; results from six different samples in 20% D_2O covering the pH range from 5.8 to 8.4 were combined and reported as their average value, pH 7.1. Results from 14 samples from pH 9.4 to 11.1 (average pH 10.3) were also combined. Results at pH 2.0, 3.5, and 13 refer to data for only the specified pH. Finally, we may estimate the overall precision of these data by computing the average standard deviations of all points from their fitted curves. One standard deviation in T_1 is ±4%, with ±7% for η. Another estimate of precision is based on the assumption that the relaxation rate, $1/T_1$, at 30 °C is a linear function of pH. The assumption is theoretically unjustified, but the fit is good (see Figure 4) with a standard deviation of ±5%.

The major sources of random error in our measurements seem to be temperature uncertainties (ca. ±2%) and spectrometer fluctuations related to signal-to-noise ratios, etc. (ca. ±3%). We have no way of estimating systematic errors since there is no T_1 standard for calibration purposes.

Results

pH Dependence. Published reports have emphasized the pH dependence of T_1 in orthophosphate solutions.[3-7] In a few preliminary runs using commercial Na_2HPO_4 (analytical reagent grade) we obtained results comparable to those of Kielman and Leyte[5] (see Figure 1); however, our results from carefully purified samples (Figure 4) show little variation with pH. Since the general features of the literature data resemble our test runs with deliberate addition of ferric ion (Figure 1), and since the other authors did not record elaborate purification procedures, we presume that their samples were contaminated with transition-metal ions.

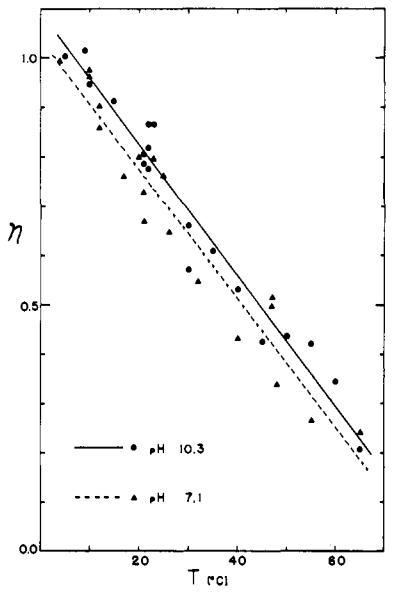

Figure 3. $^{31}P\{^1H\}$ nuclear Overhauser enhancement (η) vs. temperature for orthophosphate solutions in 20% D_2O. ^{31}P signals at 60.74 MHz were observed both with and without irradiation at 150 MHz, the solvent proton resonant frequency. Lines show the best linear fit.

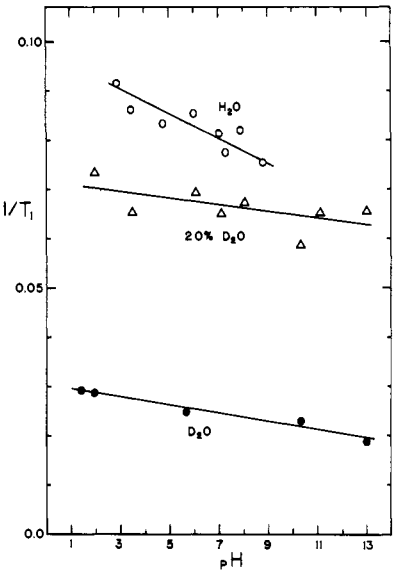

Figure 4. Relaxation rate vs. pH for sodium orthophosphate solutions: in H_2O at 24.3 MHz, 32 °C, 0.3 M; in 20% D_2O at 60.74 MHz, 30 °C, 0.10 M; in 99.8% D_2O at 60.74 MHz, 30 °C, 0.10 M. The 20% D_2O data also appear in Figure 1.

Relaxation Mechanisms. The overall relaxation rate, $R = 1/T_1$, may be resolved into contributions from individual relaxation mechanisms.

Dipole–dipole (DD) relaxation is most important at low temperature. The rate due to protons from the solvent, R^H_{DD}, is given by[14]

$$R^H_{DD} = 2\gamma_p\eta/\gamma_H T_1 = 0.8096\eta/T_1 \quad (3)$$

where γ_p and γ_H are the magnetogyric ratios of ^{31}P and ^1H,

(13) D. Canet, *J. Magn. Reson.*, **23**, 361 (1976).

(14) A. Abragam, "The Principles of Nuclear Magnetism", Oxford University Press, London, 1961.

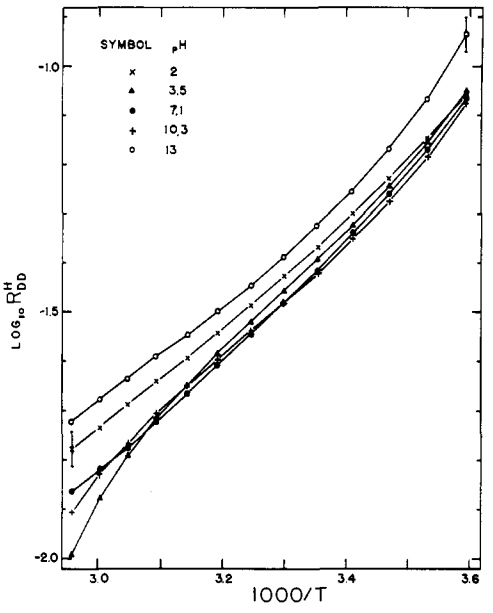

Figure 5. Dipole–dipole spin–lattice relaxation rates vs. reciprocal temperature (K^{-1}) for sodium orthophosphate solutions. Rates were calculated from ^{31}P T_1 and η measurements at 60.74 MHz. The error bars shown for selected points represent one standard deviation in the original raw data; approximately the same error limits apply to all points on the graph.

Table I. A Sample Calcualtion Illustrating the Resolution of Individual Relaxation Mechanisms

Experimental Data[a] at pH 10.3 and 25 °C			
^{31}P frequency, MHz	solvent	T_1, s ± 4%	η ± 7%[b]
40.51	100% D_2O	50.6	
60.74	20% D_2O	16.1	0.758
60.74	100% D_2O	44.6	0.064
145.75	20% D_2O	13.2	
145.75	100% D_2O	22.9	

Derived Rates, $s^{-1} \times 10^2$	20% D_2O	100% D_2O
$1/T_1$ (at 60.74 MHz)	6.22 ± 0.25	2.24 ± 0.09
R^H_{DD}[c]	3.82 ± 0.31	0.12 ± 0.01
R^D_{DD}[d]	0.06 ± 0.01	0.36 ± 0.03
R_{CSA} (at 60.74 MHz)[e]	0.29 ± 0.07	0.45 ± 0.03
R_{RES}[f]	2.05 ± 0.40	1.31 ± 0.10

[a] Obtained by least-squares fitting to experimental T_1 and η measurements as described in the text and illustrated in Figures 2 and 3. [b] Proton Overhauser effect. The NOE from nominally "100% D_2O" is due to residual protons in the commercial solvent (99.8% D_2O) as well as protons retained during lyophilization from H_2O or absorbed from the atomosphere. [c] Proton dipole-dipole relaxation rate, calculated by eq 3. [d] Deuteron dipole-dipole rate, eq 5 and 6. [e] Chemical shift anisotropy rate, eq 4. [f] Residual rate, eq 7.

respectively. This equation is valid in the fast correlation limit ($\omega^2\tau_c^2 \ll 1$) which easily applies to these solutions. Figure 5 shows the proton DD rates evaluated at 5 °C intervals from 5 to 65 °C, using eq 3 and data from the T_1 and NOE fitting functions.

Chemical shift anisotropy (CSA) is an important mechanism only at very high magnetic fields. Theoretically, the rate of this mechanism, R_{CSA}, should depend on the square of the field, or the square of the resonance frequency.[14] Our measurements at three fields follow this behavior to high precision (see data in Table I). Assuming that CSA is the only field-dependent mechanism (valid where $\omega^2\tau_c^2 \ll 1$) and that it varies strictly as the square of the resonance frequency, $R_{CSA}(\omega_1)$, the CSA rate at resonance frequency ω_1 may be calculated from T_1 measurements at two frequencies, ω_1 and ω_2:

$$R_{CSA}(\omega_1) = [1/T_1(\omega_1) - 1/T_1(\omega_2)]\omega_1^2/(\omega_1^2 - \omega_2^2) \quad (4)$$

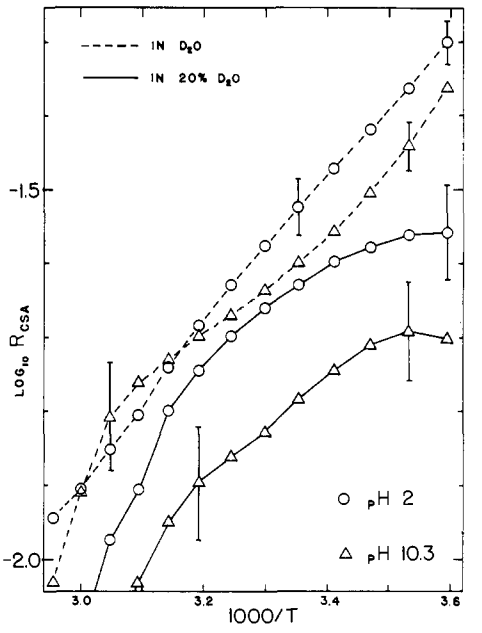

Figure 6. Chemical shift anisotropy spin–lattice relaxation rates vs. reciprocal temperature (K^{-1}). Error limits expand toward the bottom of the figure as shown for selected points.

Figure 6 shows the R_{CSA} results. Note that the error limits become quite large at high temperatures.

The residual relaxation rate, that part of the overall rate which remains after R_{DD} and R_{CS} have been subtracted, could be the sum of several other rates. One of these, the DD rate due to solvent deuterons, R^D_{DD}, was not directly accessible, since we had no way to measure the deuteron Overhauser effect, but it can be estimated from R^H_{DD}. DD rates depend[12] on $\gamma^2 I(I+1)\tau_c r^{-6}$; at any specified bond length, r, or correlation time, τ_c, deuteron rates are 6.3% as fast as relaxation from an equal number of protons. Our estimates are therefore

$$\text{for 20\% } D_2O\text{: } R^D_{DD} = 0.063R^H_{DD} \times 1/4 = 0.016R^H_{DD} \quad (5)$$

$$\text{for 100\% } D_2O\text{: } R^D_{DD} = 0.063R^H_{DD} \times 5/4 \times 1.2 = 0.095R^H_{DD} \quad (6)$$

Here the factors $^1/_4$ and $^5/_4$ reflect D/H concentration ratios. To compensate for differing correlation times, 1.2 is the approximate viscosity increase from 20 to 100% D_2O. In both eq 5 and 6, R^H_{DD} is the proton rate measured in 20% D_2O. These estimates need not be very accurate for our purpose since R^D_{DD} is always a small fraction of the total rate.

The residual rate cannot be subdivided further, nor can the mechanisms be identified by using only our experimental observations. The subject is discussed in the next section in terms of theories and models; in the present context, we simply define the residual rate as

$$R_{RES} = 1/T_1 - R_{CSA} - R^H_{DD} - R^D_{DD} \quad (7)$$

The results are displayed in Figure 7. Error limits vary considerably with temperature. To evaluate R_{RES} at pH 3.5 and 7.1, it was necessary to estimate R_{CSA}, since we did not examine all solutions at high field. Rates were assumed to be intermediate between those of pH 2 and 10.3. Errors introduced by these estimates cannot be large because R_{CSA} is much smaller than R_{RES} at 60.74 MHz.

Table I presents some data and illustrates the method used for the calculation of one point on each of Figures 5–7. The indicated error limits in the table and error bars in the figures represent the effect of one standard deviation in the original T_1 and NOE data. To some extent, the exact shapes of the curves in Figures 5–7 are artifacts of the polynomial fitting procedure used to organize the raw data; if a relaxation mechanism is a typical thermal process, a plot of log rate vs. $1/T$ should be a straight line. Table II lists activation energies, E^*, obtained from the slopes

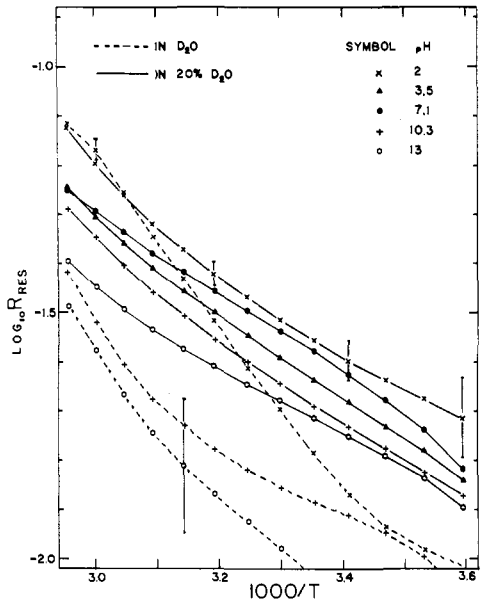

Figure 7. Residual spin-lattice relaxation rates vs. reciprocal temperature (K^{-1}). Error limits expand very rapidly for log $R_{RES} < -1.7$ as shown for selected points.

Table II. Activation Energies (kcal/mol) for Dipole-Dipole, Chemical Shift Anisotropy, and Residual Mechanisms[a]

pH	E^*_{DD}	E^*_{RES} (20% D_2O)	E^*_{RES} (D_2O)	E^*_{CSA} (D_2O)
2.0	−4.6	4.5	7.9	−4.2
3.5	−6.0	4.5		
7.1	−5.6	3.7		
10.3	−5.4	4.7	7.7	−4.8
13	−5.1	3.9	9.0	
av[b]	−5.3 ± 0.5	4.3 ± 0.4	8.2 ± 0.7	−4.5[c]

[a] Obtained by least-squares fit to the data in Figure 5-7. R_{RES} rates below 0.02 s^{-1} and R_{CSA} rates below 0.025 s^{-1} were not used in the fit because of excessive scatter. [b] Average values ± one standard deviation from the mean. [c] Estimating from the original data, the standard deviation should be about ±1.0 kcal/mol.

of lines in Figures 5–7. Error limits are standard deviations calculated from entries in the table, but it should be noted that these limits are very nearly the same as those that would have been computed from the original data. The scatter within each column of Table II appears to be random, and hence the activation energies are independent of pH within the error limits shown.

Discussion

Dipole–Dipole Relaxation. Most theories of DD relaxation resolve R_{DD} into rotational and translational (intra- and intermolecular) components. Adopting a naive view of solution dynamics, we can imagine a protonated orthophosphate ion (HPO_4^{2-} or $H_2PO_4^-$) subject to Brownian rotation in a continuous, viscous medium. Abragam[14] has shown that the rotational DD rate per proton for this simple model is given by

$$R^H_{DD}(\text{rot}) = \hbar^2\gamma_H^2\gamma_p^2\tau_r b^{-6} \quad (8)$$

at the fast correlation limit, where b is the P–H internuclear distance, and τ_r is a rotational correlation time. For a sphere of radius r in a medium with viscosity $\bar{\eta}$

$$\tau_r = 4\pi\bar{\eta}r^3/3kT \quad (9)$$

Morgan and Van Wazer[3] estimated $r = 2.22$ Å from the density of H_3PO_4, so at 25 °C $\tau_r = 1.0 \times 10^{-11}$ s. Using the structural parameters,[3,15] P–O = 1.55 Å, O–H = 1.05 Å, and ∠POH = 105°, we estimate $b = 2.09$ Å, and $R^H_{DD}(\text{rot}) = 1.1 \times 10^{-2}$ s^{-1}/proton at 25 °C. Abragam's simple model[14] for translational DD relaxation assumes Brownian diffusion through a homogeneous, viscous medium, and

$$R^H_{DD}(\text{trans}) = \hbar^2\gamma_H^2\gamma_p^2(2N/15b\bar{D}) \quad (10)$$

where N is the number density of protons in the solution ($N = 5.4 \times 10^{22}$ cm^{-3} in 20% D_2O), b is the P–H distance of closest approach, and $\bar{D}$ is an average of water molecule and phosphate ion diffusion coefficients. For water,[16] $D = 2.3 \times 10^{-5}$ cm^2 s^{-1} at 25 °C. The diffusion coefficient of phosphate may be estimated[14] from

$$D = kT/6\pi\bar{\eta}r \quad (11)$$

If $r = 2.22$ Å, then $\bar{D} = 1.7 \times 10^{-5}$ cm^2 s^{-1}, and the translational component, using $b = 2.09$ Å, is $R^H_{DD}(\text{trans}) = 6.0 \times 10^{-3}$ s^{-1} at 25 °C. The sum of the rotational and translational components is $R^H_{DD} = 1.7 \times 10^{-2}$ s^{-1} at 25 °C.

Predictions of this simple model can be compared with our data. We find the following rates at 25 °C: $R^H_{DD} \times 10^2$ (s) = 4.26, 4.06, 3.87, 3.83, and 4.74 at pH 2, 3.5, 7.1, 10.3, and 13. The rate of pH 13 does not fit the trend, probably because of ion-pairing effects which should be of major importance only in the pH 13 samples. Our results clearly do not agree with the calculations in the above paragraph. In addition, according to this model, R^H_{DD} should change by 1.1×10^{-2} s^{-1} over the narrow range near pH 7 where $H_2PO_4^-$ ions are converted to HPO_4^{2-}. We find no such change, and the magnitude of R^H_{DD} in our results is too great to be explained by either eq 8 or 10, using what we consider to be reasonable starting assumptions. Obviously, the simple model is inadequate, and relaxation is dominated by a process that is largely pH independent.

Phosphate ions have been described[17] as "structure making" because they fit nicely into the short-range tetrahedral structure of water, forming strong hydrogen bonds and tending to promote an increase in local order. According to a model originally proposed by Samoilov,[18,19] waters in the inner hydration sphere are constantly exchanging with bulk solvent. The situation is described as "positive hydration" if the "residence time" in the first hydration sphere is greater than the characteristic "jump time" in bulk solvent, i.e., the time required to diffuse a distance of one molecular diameter. A structure-making ion such as phosphate is expected to show positive hydration. Samoilov's theory suggests an alternative model for DD relaxation that is consistent with our relaxation data. We assume that the solvent around a phosphate ion is highly structured, with n protons H bonded to the oxygen atoms of the PO_4 tetrahedron. The "residence time" for each inner-sphere proton, τ_e, is the mean time before exchange with surrounding bulk waters. By analogy with eq 8, DD rates in this model are given by

$$R^H_{DD} = \hbar^2\gamma_H^2\gamma_p^2 n\tau_e b^{-6} \quad (12)$$

where b is the average inner-sphere P–H distance. Relaxation caused by protons beyond the first coordination sphere will be negligible, because of the b^{-6} dependence. Equation 12 is very similar to one derived by Hertz.[20,21] However, our model is less detailed and has fewer adjustable parameters than his. Assuming eight H bonds to each phosphate ion in 20% D_2O gives $n = 6.4$. A structure with P–O = 1.55 Å, ∠POH = 105°, and either O–H = 1.05 Å or O–H = 1.45 Å (depending on the proton's location along the H bond's double minumum potential energy curve) gives $b \simeq 2.33$ Å. R^H_{DD} from our data is 4.0×10^{-2} s^{-1}. From these numbers and eq 12 we calculate $\tau_e = 1.1 \times 10^{-11}$ s.

(15) S. N. Vinogradov and R. H. Linnell, "Hydrogen Bonding", Van Nostrand-Reinhold, Princeton, N.J., 1971.

(16) C. Devrell, *Prog. Nucl. Magn. Reson. Spectrosc.*, **4**, 235 (1969).
(17) F. Franks, Ed., "Water, a Comprehensive Treatise", Plenum Press, New York, 1975.
(18) O. Ya. Samoilov, "Structure of Aqueous Electrolyte Solutions and the Hydration of Ions", Consultants Bureau, New York, 1965.
(19) O. Ya. Samoilov in "Water and Aqueous Solutions: Structure, Thermodynamics and Transport Processes", R. A. Horne, Ed., Wiley-Interscience, New York, 1972, Chapter 14.
(20) A. Geiger and H. G. Hertz, *J. Solution Chem.*, **5**, 365 (1976).
(21) R. G. Bryant, *Annu. Rev. Phys. Chem.*, **29**, 167 (1978).

This is a reasonable result. The residence time, τ_e, is longer than the structural relaxation time for bulk water molecules[16,22] (ca. 2×10^{-12} s) as measured by ultrasonic absorption or the jump diffusion time ($\tau_j = 1.7 \times 10^{-12}$ s) measured by neutron inelastic scattering. The two methods measure closely related properties.[22] Samoilov's theory with positive hydration requires $\tau_e > \tau_j$. The calculated value of τ_e is long enough to imply the existence of a well-developed H-bonding network describing a definite structure surrounding the PO_4. The main difference between our model and the similar one developed by Hertz[20,21] is that Hertz assumed a continuous but nonuniform distribution of protons throughout the medium. His theory is particularly appropriate for ions with negative hydration. We prefer our model in the present case because we require a structurally oriented model to explain all our results (vide infra) and because, after assuming a definite structure, fewer adjustable parameters are needed. The magnitude of τ_e is also comparable to the rotational correlation time of a "free" phosphate ion calculated from eq 9, but this is only a coincidence. The preferred model with multiple strong hydrogen bonds does not allow for rapid free rotation of the phosphate group. Ordinarily, the longer correlation time of a hydrated phosphate would lead to faster relaxation than that observed. However, since the protons reside at the phosphate only for a shorter time, τ_e, the rotational correlation mechanism is effectively decoupled. Hence, the relaxation rate should be largely pH independent as was found.

Samoilov's theory[18,19] predicts a correlation time given by

$$\tau_e = \tau_j e^{\Delta E/RT} \tag{13}$$

where τ_j is the jump diffusion time of bulk water and ΔE is the height of an additional barrier which hinders the motion of water molecules near the ion. According to this model, the overall activation energy for DD relaxation is the activation energy for τ_e:

$$E^*_{DD} = -(E_j^* + \Delta E) \tag{14}$$

The activation energy for structural relaxation, E_j^*, is 4.1 kcal/mol.[22] Equations 13 and 14 with $\tau_e = 1.1 \times 10^{-11}$ and $\tau_j = 1.7 \times 10^{-12}$ at 25 °C predict $E^*_{DD} = -5.2$ kcal/mol, which may be compared to our measured value (Table II) of -5.3 ± 0.5 kcal/mol.

Relaxation by Chemical Shift Anisotropy. Spin–lattice relaxation can occur when the local environment provides a fluctuating chemical shift to the ^{31}P nucleus. This CSA mechanism is most commonly seen in a rapidly tumbling molecule that has an anisotropic shielding tensor. For an axial tensor the rate is[14]

$$R_{CSA} = (2/15)\omega_p^2(\Delta\sigma)^2\tau_r \tag{15}$$

where ω_p is the ^{31}P angular precessional frequency, $\Delta\sigma$ is the fractional difference between extreme values of the shielding tensor, and τ_r is a rotational correlation time, usually calculated from eq 9.

All protonated phosphate ion species are anisotropic; $\Delta\sigma$ has not been measured, but ab initio molecular orbital calculations predict[24] that $\Delta\sigma = 163 \times 10^{-6}$ for $H_2PO_4^-$. These theoretical results refer to isolated ions and are therefore not exactly appropriate for aqueous phosphate solutions. However, eq 15 with the theoretical $\Delta\sigma$ and our data from Figure 6 ($R_{CSA} = 3.0 \times 10^{-2}$ s^{-1} in D_2O at 25 °C, pH 2, and 145.75 MHz) give $\tau_r = 1.0 \times 10^{-11}$ s. In 20% D_2O under the same conditions, $\tau_r = 8.8 \times 10^{-12}$ s. At 5 °C we find a more dramatic solvent effect: in D_2O $\tau_r = 1.7 \times 10^{-11}$ s while in 20% D_2O $\tau_r = 1.0 \times 10^{-11}$ s.

Our results are inconsistent with the usual CSA relaxation process (unless $\Delta\sigma$ is greatly in error) because the calculated τ_r values above are too short to represent physical rotation of the phosphate ion. An explanation can be found, however, in terms of our inner-sphere hydrogen-bonding model. Hydrogen bonds consist of a proton or deuteron confined to a double minimum potential energy well.[15] Leuchs and Zundel,[25] using infrared techniques, have shown that the wells between water and a phosphate ion are nearly symmetrical. The eight inner-sphere hydrogen bonds in our model were assumed to be equivalent, even though at any instant one or two protons occupy the inner minimum. Obviously the model requires a rapid oscillation across the low potential barriers. The fastest translation process in water is proton conduction which takes place by proton exchange through chains of hydrogen-bonded water molecules. Protonated phosphate ions could also participate in this process. A solvated HPO_4^{2-} could shift its unique inner proton toward a neighboring water molecule while simultaneously (or almost simultaneously) receiving a proton along another of its hydrogen bonds. The net effect of this process, which we call quasi-rotation, is to "rotate" the site of attachment (and the chemical shielding tensor) without physically rotating the PO_4 structure.

Rotational correlation times may be defined as the mean time required for an object to rotate through 1 rad. Since tetrahedral angles are approximately 1 rad, we identify our measured τ_r as being the mean quasi-rotation jump time. τ_r in our model could not be longer than τ_e in eq 12; otherwise some protons remain attached to the phosphate for times longer than τ_e and the concept of DD relaxation by eight equivalent protons would have to be modified.

Quasi-rotation is potentially a very fast process. The masses involved and the distances they must move are very small. These considerations lead us to propose that quantum-mechanical tunneling[15,26,27] is the probable explanation for the solvent effect. The results shown in Figure 6 appear to show that proton quasi-rotation in 20% D_2O leads to a low-temperature limiting value for R_{CSA}. A curve such as this with zero slope at low temperature is characteristic of tunneling. Tunneling rates are also very sensitive to mass; the nearly constant slope in D_2O indicates that deuteron tunneling occurs at negligible rates. Busch and de la Vega[26] argue that very rapid proton tunneling must be expected in highly symmetrical H bonds (as in ice) with rates approaching 10^{13} s^{-1}; the introduction of even slight asymmetry (e.g., in water) can lower the tunneling rate by orders of magnitude. Our results fall within the range of tunneling rates observed in other H-bonded systems.[15]

Relaxation by Quasi-Spin Rotation. The residual relaxation rates (Figure 7 and Table II) show positive activation energies. Following the usual practice we could assign R_{RES} to a spin rotation (SR) mechanism. SR is commonly regarded as the only mechanism with a positive activation energy; indeed, it is difficult to identify by any other criterion. Nevertheless, we reject the SR assignment for the following reasons.

(1) To be entirely consistent with SR theory, a model must allow short intervals of free rotation, interrupted by frequent collisions and abrupt changes in angular velocity.[28] According to our H-bond model, a PO_4 unit is locked into the local solvent structure. Slow diffusive rotation must occur, of course, but "free" rotation cannot be accommodated.

(2) No SR theory can explain the solvent dependence of our activation energies. We find very different E^*_{RES} in D_2O and in 20% D_2O.

Another mechanism with a positive activation energy is needed. This could be a pulse mechanism. Imagine a series of pulse events of equal amplitude and very short duration that occur at random times. Each pulse has a certain probability of causing spin relaxation independent of the effects of other pulses, so a faster pulse rate means a greater relaxation rate. Any thermally driven pulse process likely has a greater rate at higher temperatures, i.e., a positive activation energy.

The quasi-rotation process discussed above may be associated with a suitable pulse mechanism. When the inner H bond flips

(22) C. M. Davis and J. Jarzynski, in ref 19, Chapter 10.
(23) J. Jonas, T. De Fries, and D. J. Wilbur, *J. Chem. Phys.*, **65**, 582 (1976).
(24) F. R. Prado, C. Giessner-Prettre, B. Pullman, and J.-P. Daudley, *J. Am. Chem. Soc.*, **101**, 1737 (1979).
(25) M. Leuchs and G. Zundel, *Can. J. Chem.*, **57**, 487 (1979).
(26) J. H. Busch and J. R. de la Vega, *J. Am. Chem. Soc.*, **99**, 2397 (1977).
(27) O. Tapia and E. Poulain, *Int. J. Quantum Chem.*, **11**, 473 (1977).
(28) D. W. G. Smith and J. G. Powles, *Mol. Phys.*, **10**, 451 (1966).

from one oxygen to another, there will be an almost instantaneous electric charge redistribution. Not only a proton or deuteron but also a negative charge undergoes quasi-rotation, and the resulting pulse of electron current through the ion may generate an electromagnetic pulse capable of relaxing the nuclear spin. We call this mechanism quasi-spin rotation (QSR).

QSR may be analyzed by using concepts from FT NMR.[29] An electromagnetic pulse rotates the spin magnetization vector through an angle α:

$$\alpha = \gamma_p H_{x,y} \tau_w \quad (16)$$

where $H_{x,y}$ is the effective pulse amplitude (a field with x and y axis components) and τ_w is the pulse width. Our pulses have amplitude H and occur at random orientations to the external field. Since H_z components are ineffective

$$H_{x,y}^2 = H_x^2 + H_y^2 = (2/3)H^2 \quad (17)$$

The fractional change in z-axis magnetization induced by a weak pulse is given by (for small α)

$$\Delta M_z/M_z = 1 - \cos\alpha \simeq (1/2)\alpha^2 \quad (18)$$

Equation 18, applied to FT NMR, describes a change in bulk magnetization involving an entire spin ensemble. In our mechanism, each pulse interacts with only one spin, and eq 18 describes the probability that a single QSR pulse relaxes that spin. The QSR relaxation rate from eq 16, 17, and 18 is

$$R_{QSR} = (\Delta M_z/M_z)/\Delta t = (1/3)\gamma_p^2 H^2 \tau_w^2 \tau_r^{-1} \quad (19)$$

where τ_r may be identified as the quasi-rotation jump time of eq 15.

The following order of magnitude calculation indicates that eq 19 can account for the observed rate. Assume that when a proton quasi-rotates, the pulse generates a field equivalent to one Bohr magneton, β, at a distance of 1 Å from the ^{31}P nucleus. Then $H^2 = \beta^2/(1\ \text{Å})^6 \simeq 10^8\ G^2$. Let the pulse width be the time required for a proton to jump between the H-bond double minima, or approximately the oscillation period of a proton in a hydrogen bond, $\tau_w = 10^{-14}$ s. If $\tau_r = 10^{-11}$ s, then eq 19 gives $R_{QSR} \simeq 3 \times 10^{-2}\ s^{-1}$, in agreement with our data for R_{RES}.

An interesting relationship is obtained by multiplying eq 19 and 15:

$$R_{CSA}R_{QSR} = (2/45)\omega_p^2(\Delta\sigma)^2\gamma_p^2H^2\tau_w^2 \quad (20)$$

The temperature-dependent term, τ_r, is canceled. We have tested eq 20 with our data, using $R_{RES} = R_{QSR}$. Unfortunately, our data are not ideally suited for this purpose. At high temperatures, where R_{RES} is accurately known, R_{CSA} is quite uncertain; at low temperatures the reverse is true. Nevertheless, the following averages result from using data over the most reliable range (10–50 °C). At pH 10.3 and 145.75 MHz, $R_{CSA}R_{RES} \times 10^4 = 3.5 \pm 0.5$ in D_2O and 3.3 ± 0.7 in 20% D_2O, and the activation energies in both solvents were zero within experimental error (0.1 ± 0.6 and 0.3 ± 1.0 kcal/mol). At pH 2 the average combined rates ($\times 10^4$) were 5.5 ± 1.2 in D_2O and 7.0 ± 1.4 in 20% D_2O, with identical activation energies (-0.8 ± 1.0 kcal/mol) in both solvents.

The results above confirm our expectation that temperature effects are small or absent in eq 20. There is also no significant solvent isotope effect, even though it is quite important in both R_{CSA} and R_{QSR} alone. Solvent isotope effects on E^*_{RES} and E^*_{CSA} enter through τ_r which includes a major contribution due to tunneling in 20% D_2O but not in 100% D_2O. Equation 20 will be insensitive to isotope effects if the pulse angle α depends only on the quantity of charge shifted during a pulse; i.e., if the isotope effects on H^2 and τ_w^2 are opposite and cancel. This leaves $\Delta\sigma$ as the only real variable in eq 20. We interpret pH effects on $(R_{CSA}R_{RES})$ to show that $\Delta\sigma$ varies as the phosphate ion is protonated. $\Delta\sigma$ is greater for $H_2PO_4^-$ (at pH 2) than for HPO_4^{2-} (at pH 10.3).

Acknowledgments. Work on this project was begun at the Lawrence Berkeley Laboratory. One of the authors (J.L.M.) thanks Dr. M. P. Klein for his advice and kind hospitality and Drs. I. Salmeen and N. Teng for their assistance and encouragement. The authors are grateful to Dr. R. E. Santini for designing and optimizing some of the NMR instrumentation. This investigation was supported by National Institutes of Health Research Grant RR01077 from the Division of Research Resources.

(29) D. Shaw, "Fourier Transform NMR Spectroscopy", Elsevier, Amsterdam, 1976.

Interaction of *cis*-$[Pt(NH_3)_2(H_2O)_2](NO_3)_2$ with Ribose Dinucleoside Monophosphates[1]

J. C. Chottard,*[2a] J. P. Girault,[2a] G. Chottard,[2c] J. Y. Lallemand,[2b] and D. Mansuy[2a]

Contribution from the Laboratoire de Chimie de Coordination Organique et Biologique and Laboratoire de Résonance Magnétique Nucléaire, Laboratoire de Chimie de l'Ecole Normale Supérieure, Associé au CNRS, 75231 Paris Cedex 05, France, and Département de Recherches Physiques, Associé au CNRS, Université Pierre et Marie Curie, 75230 Paris Cedex 05, France.
Received December 10, 1979

Abstract: The reactions of five dinucleoside monophosphates (IpI, GpG, ApA, GpC, and ApC) with *cis*-$[Pt(NH_3)_2(H_2O)_2](NO_3)_2$, with both reactants ca. 4×10^{-4} M in water (pH 5.5), have been studied. Sephadex chromatography and LC, ^1H NMR, and CD analyses have been used to characterize the complexes formed. The three homodinucleotides have a geometry leading to N(7)–N(7) chelation of the metal. IpI and GpG give a single N(7)–N(7) chelated complex while ApA also gives other products due to competitive N(1) binding to the metal. GpC and ApC lead to mixtures of several complexes and in both cases cytosine appears to have more affinity for the platinum than do guanine and adenine. In the case of GpC one of the complexes appears as an N(7)G–N(3)C platinum chelate, the CD of which supports a left-handed helical arrangement of the bases. As far as the perturbation of the DNA structure upon binding of the *cis*-$(NH_3)_2Pt^{II}$ moiety is concerned, these results bring further support to the hypothesis of intrastrand cross-linking of adjacent guanines occurring after a local denaturation or premelting of the DNA. They also suggest that cross-linking of adjacent guanine and cytosine could occur for a left-handed sequence of the polynucleotide.

The mechanism of action of the antitumor *cis*-dichlorodiammineplatinum(II) complex[3] is still the subject of active investigations.[4,5] There is much evidence which suggests that DNA is the primary target of the platinum(II) drug.[6-9] Several studies

0002-7863/80/1502-5565$01.00/0